

# Generation and validation of a zebrafish model of EAST (epilepsy, ataxia, sensorineural deafness and tubulopathy) syndrome

Fahad Mahmood<sup>1,\*</sup>, Monika Mozere<sup>2,\*</sup>, Anselm A. Zdebik<sup>2,3,\*</sup>, Horia C. Stanescu<sup>2,4</sup>, Jonathan Tobin<sup>4</sup>, Philip L. Beales<sup>4</sup>, Robert Kleta<sup>2,3,4,‡</sup>, Detlef Bockenhauer<sup>2,4,‡</sup> and Claire Russell<sup>1,‡,§</sup>

## SUMMARY

Recessive mutations in *KCNJ10*, which encodes an inwardly rectifying potassium channel, were recently identified as the cause of EAST syndrome, a severe and disabling multi-organ disorder consisting of epilepsy, ataxia, sensorineural deafness and tubulopathy that becomes clinically apparent with seizures in infancy. A *Kcnj10* knockout mouse shows postnatal mortality and is therefore not suitable for drug discovery. Because zebrafish are ideal for *in vivo* screening for potential therapeutics, we tested whether *kcnj10* knockdown in zebrafish would fill this need. We cloned zebrafish *kcnj10* and demonstrated that its function is equivalent to that of human *KCNJ10*. We next injected splice- and translation-blocking *kcnj10* antisense morpholino oligonucleotides and reproduced the cardinal symptoms of EAST syndrome – ataxia, epilepsy and renal tubular defects. Several of these phenotypes could be assayed in an automated manner. We could rescue the morphant phenotype with complementary RNA (cRNA) encoding human wild-type *KCNJ10*, but not with cRNA encoding a *KCNJ10* mutation identified in individuals with EAST syndrome. Our results suggest that zebrafish will be a valuable tool to screen for compounds that are potentially therapeutic for EAST syndrome or its individual symptoms. Knockdown of *kcnj10* represents the first zebrafish model of a salt-losing tubulopathy, which has relevance for blood pressure control.

## INTRODUCTION

Recently, we and others elucidated the pathophysiological basis of a multisystem disorder characterised by infantile-onset epilepsy, debilitating ataxia, sensorineural deafness and a salt-wasting tubulopathy, i.e. EAST syndrome (Bockenhauer et al., 2009; Scholl et al., 2009). Current treatment for this disorder caused by malfunction of the potassium channel *KCNJ10* in affected organs is non-specific and unsatisfactory. *KCNJ10*, expressed in the distal tubule of the kidney in humans and mice (Bockenhauer et al., 2009; Reichold et al., 2010), indirectly modulates renal tubular sodium reabsorption by recycling potassium (K<sup>+</sup>) (Bleich, 2009; Bockenhauer et al., 2009). Mutations in *KCNJ10* therefore result in a salt-losing tubulopathy (Bandulik et al., 2011; Bockenhauer et al., 2009). In the central nervous system (CNS), *KCNJ10* is predominantly expressed in glial cells of the cerebral cortex and cerebellar cortex, where *KCNJ10* helps to buffer extracellular K<sup>+</sup>

and thus modulates neuronal excitability (Olsen and Sontheimer, 2008), with channel malfunction likely leading to epilepsy and ataxia. In the inner ear, *KCNJ10* is expressed in the stria vascularis, where it has been proposed to generate the endocochlear potential (Hibino et al., 1997), and in the satellite cells that ensheath the auditory nerve (Hibino et al., 1999). However, the specific cause(s) of deafness in individuals with EAST syndrome are still unclear (Rozenfurt et al., 2003). *KCNJ10* is also expressed in the retina, and patients show specific electroretinographic changes (Thompson et al., 2011).

*Kcnj10* knockout mice replicate key symptoms of the human disease, but additionally have CNS vacuolation and neonatal death (Neusch et al., 2001). These features obviously impair the testing of novel therapeutic approaches, including drug discovery and testing. Hence, new models of EAST syndrome must be developed, which are more amenable to therapeutic testing and drug discovery. Because EAST syndrome shares several symptoms with other diseases, such as epilepsy and ataxia, any novel therapeutic drugs found using a model of EAST syndrome could also be beneficial to individuals suffering from these common and debilitating symptoms. It might also be a suitable model to study drugs affecting renal salt handling, which are of significant interest for modulation of blood pressure.

Zebrafish (ZF; *Danio rerio*) are genetically tractable, can be studied at low cost, and large numbers can be exposed to potential therapeutics simultaneously. They are thus ideally suited for *in vivo* screening of potential therapeutic compounds (Hortopan et al., 2010b; Parg et al., 2002). We therefore generated *kcnj10* morphant ZF as a model for EAST syndrome. These fish recapitulate key features of EAST syndrome, including seizures, ataxia and renal tubular defects, establishing *kcnj10* morphants as the first validated ZF model of a tubulopathy.

<sup>1</sup>Department of Comparative Biomedical Sciences, Royal Veterinary College, London, UK

<sup>2</sup>Centre for Nephrology, University College London, London, UK

<sup>3</sup>Departments of Neuroscience, Physiology and Pharmacology, University College London, London, UK

<sup>4</sup>Institute of Child Health, University College London, London, UK

\*<sup>‡</sup>These authors contributed equally to this work

<sup>§</sup>Author for correspondence (crussell@rvc.ac.uk)

Received 27 December 2011; Accepted 2 January 2013

© 2013. Published by The Company of Biologists Ltd  
This is an Open Access article distributed under the terms of the Creative Commons Attribution Non-Commercial Share Alike License (<http://creativecommons.org/licenses/by-nc-sa/3.0/>), which permits unrestricted non-commercial use, distribution and reproduction in any medium provided that the original work is properly cited and all further distributions of the work or adaptation are subject to the same Creative Commons License terms.

## TRANSLATIONAL IMPACT

### Clinical issue

Individuals with EAST syndrome suffer from a debilitating disease characterised by epilepsy, ataxia, sensorineural deafness and renal tubulopathy. There is no cure and the currently available treatments are not always effective. The cause was only recently identified as recessive mutations in *KCNJ10*. To test potential therapeutics, suitable disease models are needed. Because the mouse *Kcnj10* knockout has a much more severe phenotype (including brain dysmorphology and neonatal death) than humans with EAST syndrome, it is not an ideal model. Here, the authors set out to develop a model of EAST syndrome using zebrafish, because zebrafish embryos and larvae are ideal for *in vivo*, high-throughput drug discovery.

### Results

The authors identified and cloned *kcnj10*, the zebrafish homologue of human *KCNJ10*, and used antisense technology to knock down its expression in zebrafish during embryonic and larval stages. These fish were viable and did not exhibit brain dysmorphology. Similar to humans with EAST syndrome, *kcnj10* knockdown fish showed phenotypes such as epilepsy, ataxia and renal tubulopathy. This phenotype was rescued by normal but not mutated human *KCNJ10*, indicating functional equivalence. These phenotypes are useful for drug discovery because their detection can be automated.

### Implications and future directions

Given that phenotypes observed in this new zebrafish model of EAST syndrome can be detected in an automated manner, this model is ideal for *in vivo* drug discovery, and could accelerate the discovery of drugs for this syndrome. Such drugs might also be effective treatments for other potassium channelopathies or diseases with similar symptoms. Zebrafish expressing human mutant *KCNJ10* provide a tool to identify drugs that specifically modulate the function of human mutant *KCNJ10*, which could enable the development of personalised treatments for individuals with EAST syndrome with specific mutations. In addition, to the authors' knowledge, this is the first reported zebrafish model of renal tubulopathy, meaning it could provide a platform for drug discovery for renal tubulopathy.

## RESULTS

### Identification and cloning of zebrafish *kcnj10*

Over the past 4 years, we have searched various databases from the *Danio rerio* sequencing projects for ZF *kcnj10*. Initially, a BLAST search using the human protein *KCNJ10* on ZF reference sequence (RefSeq) produced XP\_001342993 as the best hit (with a predicted open reading frame resulting in a 425 amino acid protein). On the basis of this homology and conservation of chromosomal arrangements of the *KCNJ* gene family, we conclude that the *KCNJ9-KCNJ10* pair on human chromosome 1 is the equivalent of a ZF region situated on chromosome 7 (see Materials and Methods for details). This includes the *KCNJ10* orthologue ENSDARG00000090815 (ENSEMBL zv9). Henceforth, we refer to this gene as *kcnj10a*.

Subsequently, the ENSEMBL database also labelled a second gene as a potential *KCNJ10* orthologue and this gene has received the label ENSDARG00000014697. We also investigated this second gene (see below), to which we will henceforth refer to as *kcnj10b*.

We first amplified the 5' untranslated region of ZF *kcnj10a* by PCR from random-primed complementary DNA (cDNA) and an in-frame stop codon was identified upstream of the start codon (Fig. 1A). We next cloned the entire coding region of this ZF orthologue of human *KCNJ10*, and sequencing confirmed that it has 68% identity and 80% similarity at the protein level (Fig. 1B). Conservation of the first three amino acids further confirmed the

likely start codon. In order to prove its function, we expressed ZF *Kcnj10a* in *Xenopus* oocytes and observed barium-sensitive, inwardly rectifying and K<sup>+</sup>-selective currents that closely resembled human *KCNJ10* (Fig. 1C-E) (Reichold et al., 2010).

### Expression pattern in zebrafish

We next examined the spatio-temporal expression of *kcnj10a* mRNA from the 128-cell stage to 120 hpf (hours post fertilization) by *in situ* hybridisation in wild-type (WT) ZF. At stages up to 24 hpf, expression was not detectable, but from 48-120 hpf there was prominent expression of *kcnj10a* in the brain and spinal cord (Fig. 2A-F). We examined the expression at 120 hpf in detail (Fig. 2G-O). Expression in the brain and spinal cord was adjacent to ventricles (e.g. 'v' in Fig. 2J, 'sc' in 2N), where glial cell bodies are located. In the retina, expression was within the inner nuclear layer (Fig. 2I), where Müller glia reside. These sites of expression are therefore consistent with glial cell bodies (Marcus and Easter, 1995), but not neurons (Mueller and Wullimann, 2005). We also found *kcnj10a* expression in ZF organs equivalent to those affected by EAST syndrome, namely cerebellum ('cp' in Fig. 2E,K), otic vesicles ('ov' in Fig. 2L, enlarged in 2M), pronephros ('p' in Fig. 2G, enlarged in 2H,O) and retina ('r' in Fig. 2I). *In situ* hybridisation in ZF with a sense control riboprobe under the same conditions did not show any specific staining (supplementary material Fig. S1A).

We also examined the spatio-temporal expression of *kcnj10b* mRNA from 24 hpf to 120 hpf by *in situ* hybridisation in WT ZF (supplementary material Fig. S2). We could not detect expression until 30 hpf (supplementary material Fig. S2A), at which point it was ubiquitous in the CNS until 48 hpf (supplementary material Fig. S2B). By 72 hpf, the expression remained ubiquitous throughout the brain but was increased adjacent to the ventricles and in the axon tracts of the midbrain and hindbrain (supplementary material Fig. S2C), and became more restricted up to 120 hpf (supplementary material Fig. S2D-G), including in the cerebellum (arrow in supplementary material Fig. S2F). Expression of *kcnj10b* was seen in the otic vesicle at 120 hpf but not in the pronephros or spinal cord. The riboprobe was specific: the sense probe did not produce any signal (supplementary material Fig. S1B).

### Knockdown of ZF *kcnj10a*

We designed two antisense morpholino oligonucleotides (MOs), one against a donor splice site (intron 2) and the other against the start codon of *kcnj10a*. We confirmed efficacy of the splice site MO by performing PCR on cDNA prepared from RNA extracted from WT and morphant fish. Amplification of *kcnj10a* showed that 39 bp from the end of exon 2 (partly encoding a transmembrane region critical for the function of *Kcnj10a*) were missing in the morphant cDNA (supplementary material Fig. S3).

Fish injected with 0.5-2 ng of either MO, but not a control MO, looked normal but displayed abnormal movements, so this amount of MO was used for subsequent experiments. The earliest phenotype was a statistically significant increase in frequency of spontaneous contractions (Fig. 3A). Early phenotypes are more likely to be rescued by co-injected cRNA. Indeed, when we co-injected human WT cRNA together with the splice site MO, the frequency of spontaneous contractions returned to normal levels, whereas cRNA containing the human R65P mutation, associated with EAST syndrome, did not rescue the morphant phenotype

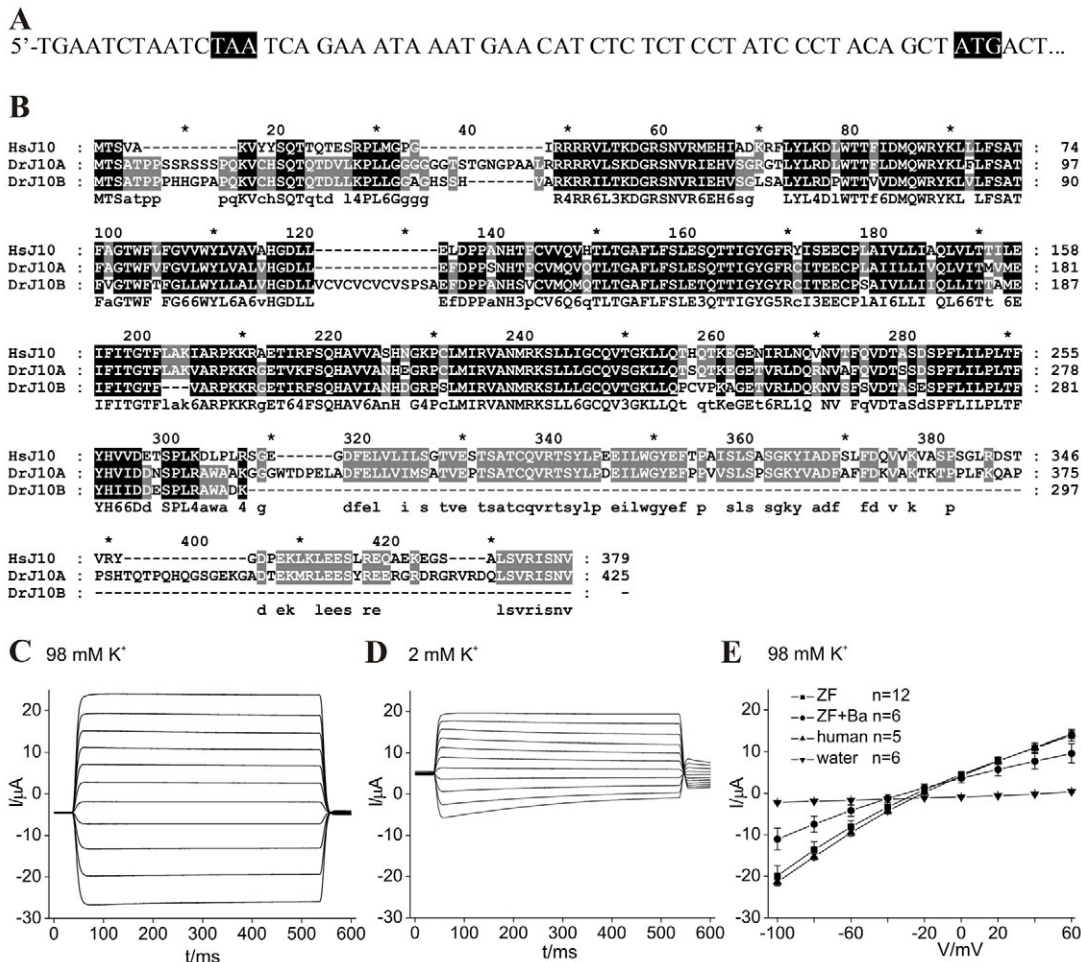


**Fig. 1. Identification and function of ZF *kcjn10*.** (A) The 5' end of ZF *kcjn10a* cDNA. The start codon and the first upstream stop codon are highlighted. (B) Alignment of the Kcnj10a and Kcnj10b protein sequences from ZF (DrJ10A and DrJ10B) and human (HsJ10) shows the high similarity between the orthologues. Black shows sequences that are identical in all three proteins; grey shows sequences that are identical in two of the proteins. (C-E) Heterologous expression of ZF *Kcnj10a* in *Xenopus laevis* oocytes results in K<sup>+</sup>-selective currents. Currents were obtained by two-electrode voltage clamp with voltage steps from -100 to +60 mV with 98 mM KCl (C) or 2 mM KCl (D) in the bath solution and were superimposed. C and D depict typical experiments, whereas the averaged current-voltage (*I*-*V*) traces from all data are shown in E, with data from oocytes injected with water or human *KCNJ10* for comparison. These current-voltage traces reflect the average currents obtained 50 ms after the cells were clamped to the voltage steps indicated above. Currents were nonlinear, i.e. inwardly rectified, in keeping with the properties of currents mediated by human *KCNJ10*. This characteristic property is attributed to pore block by intracellular cations, which only affects outward currents. Ba, barium.

(Fig. 3A). Thus, human and ZF *KCNJ10* are functionally equivalent. Furthermore, this model therefore enables the effect of drugs to be tested on various human mutant *KCNJ10*.

### Movement defects in *kcjn10a* morphant ZF

Because EAST syndrome is characterised by ataxia and epilepsy, we examined morphant movement in detail. In addition to an increased frequency of spontaneous contractions at 30 hpf (Fig. 3A), which could indicate that neurons are hyperexcitable, several other abnormal movement phenotypes were detected in *kcjn10a* morphants at 120 hpf. Locomotion tracking of swimming during the touch-evoked escape response was characterised by frequent circling or loops around the morphant's vertical axis (Fig. 3C,D), which was not seen in WT ZF. Movies of free-swimming larvae demonstrated that swimming was laboured and morphants

struggled to maintain an upright posture, with excessive fin movements that did not accompany locomotion, which we interpret as ataxia. On occasions, larvae would have a burst of speed, usually in one direction so they would continue to try to swim forward even when they hit the wall of the dish, followed by a sudden and complete loss of posture [supplementary material Movies 1 (WT) and 2 (*kcjn10a* morphant)]. This phenotype has been described before for ZF larvae having seizures (Baraban et al., 2005; Hortopan et al., 2010a). *kcjn10a* morphants also showed abnormal facial movements characterised by more frequent eye and jaw movements, often only on one side, another indication of ataxia [supplementary material Movies 1 (WT), 2 and 3 (*kcjn10a* morphant); Fig. 3B]. To examine the locomotion phenotype more closely, we performed locomotion tracking on 120-hpf larvae and found that, overall, *kcjn10a* morphants did not swim as far in the

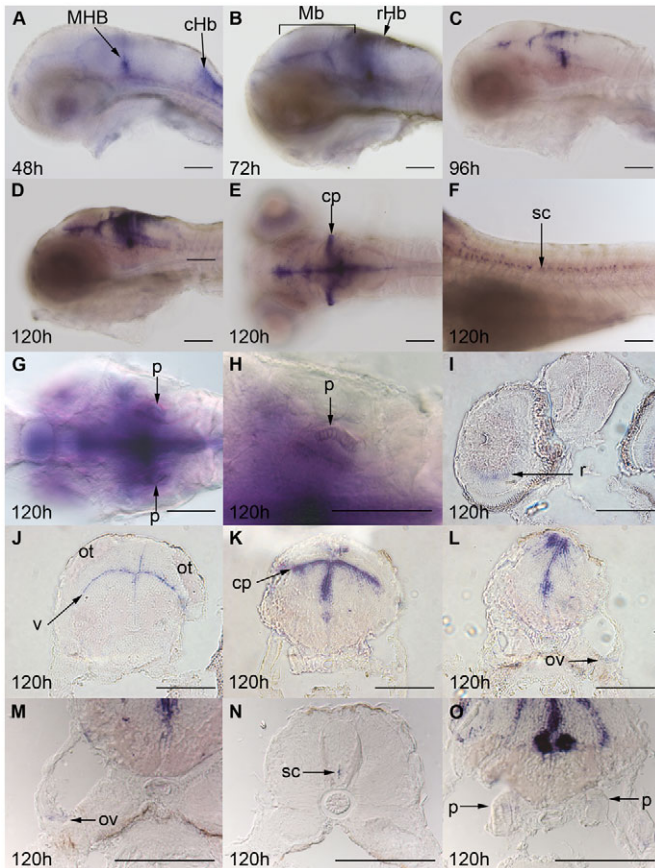


**Fig. 2. ZF *kcnj10a* is expressed in brain, otic vesicles and pronephros.** At 24 hpf, *kcnj10a* expression cannot be detected by *in situ* hybridisation (not shown) but, by 48 hpf (A), *kcnj10a* is expressed strongly in the mid-hindbrain boundary (MHB) and caudal hindbrain (cHb), and weakly in the midbrain and rostral hindbrain. (A-F) Until 120 hpf, *kcnj10a* expression becomes stronger, especially in the midbrain and rostral hindbrain (see Mb and rHb labels in B), and in the cerebellum (cp in E). More posteriorly, expression can be seen in the spinal cord (sc in F), but there is no evidence of expression in the lateral line. (I-O) Transverse sections at 120 hpf demonstrate *kcnj10a* expression in the inner nuclear layer of the retina (r in I) and reveal the majority of midbrain (J), hindbrain (K,L,M) and spinal cord (N) expression to be adjacent to the ventricles (for example, v in J). *kcnj10a* is also expressed in the cerebellum (cp in E,K), otic vesicle (ov in L,M) and weakly in the pronephros (p in G,H,O). (A-H) Whole-mount embryos with H being a higher magnification image of the pronephros (p) shown in G. (A-D,F) Lateral views with anterior to the left and dorsal up. (E,G,H) Dorsal views with anterior to the left. (I-L) Progressively more posterior transverse sections. (M-O) Higher magnification images of the otic vesicle, spinal cord and pronephros. ot, optic tectum. Scale bars: 100  $\mu$ m.

same length of time as WT or *p53* morphant larvae (supplementary material Fig. S4B).

To examine whether these locomotion defects could be due to morphological defects in the nervous system, we examined axons in 120-hpf larvae by using anti-acetylated  $\alpha$ -tubulin immunohistochemistry. We found no defects in *kcnj10a* morphants in any part of the central or peripheral nervous system, including the cerebellum, retina, optic vesicle, lateral line and motor neurons (supplementary material Fig. S5), suggesting that the locomotion

defects we see are due to physiological defects caused by loss of *Kcnj10a*.

### The phenotype is specific for *kcnj10a* MO

We also examined whether the movement disorder could be due to off-target toxic effects of the MO. To this end, we co-injected *kcnj10a* MO and *p53* MO (8 ng). Co-injection with *p53* MO had no effect on the number of tail flicks at 30 hpf or the total distance swam at 120 hpf (supplementary material Fig. S4A,B).

### Knockdown of ZF *kcnj10b*

An antisense MO against the start codon of *kcnj10b* was designed and embryos were injected with 2–8 ng. We found that this MO caused a striking phenotype at 24 hpf, with embryos being much smaller and abnormal. To test whether this phenotype was due to off-target toxic effects, we co-injected 8 ng *p53* MO and found that the phenotype remained, albeit slightly weaker (supplementary material Fig. S6A–D). Locomotion assays on *kcnj10b* morphants and *kcnj10b/p53* double morphants were non-informative owing to the severe anatomical abnormalities.

### Kidney defects in *kcnj10a* morphant ZF

Individuals with EAST syndrome also suffer from a renal tubular defect resulting in hypokalemic metabolic alkalosis and hypomagnesemia. We examined the pronephric duct and found that it was dilated in *kcnj10a* morphants compared with WT. This was often accompanied by pericardial edema, probably caused by water retention (Fig. 4A,B). We directly tested the ability of morphants to excrete water by injecting fluorescent dextran and monitoring its levels in the body immediately after injection, and again after 24 hours. In WT ZF, 91% was excreted by the kidney within 24 hours, compared with only 26% for morphants (Fig. 4E).

## DISCUSSION

We present here a validated ZF model of EAST syndrome that shows phenotypes suitable for automated detection during *in vivo* drug discovery. First, we identified the orthologue of human *KCNJ10* in ZF. Next, we proved that the identified ZF *kcnj10a* is appropriately expressed, encodes a functional potassium channel and that this channel is functionally equivalent to human *KCNJ10*. Finally, we show that *kcnj10a* morphants recapitulate key features of EAST syndrome seen in man.

Identification of the correct ZF *kcnj10* is the first important result of this study. Currently, ENSEMBL (Zv9) identifies two genes, ENSDARG00000014697 and ENSDARG00000090815, as potential orthologues of human *KCNJ10*. However, several lines of evidence presented here argue for ENSDARG00000090815 as the relevant orthologue: (1) the chromosomal localisation of ENSDARG00000090815 retains the evolutionary conservation of tandem pairs of genes encoding KCNJ channels. (2) ENSDARG00000090815 is expressed in the key organs involved in EAST syndrome. (3) MOs against ENSDARG00000090815 recapitulate key features of EAST syndrome. (4) The phenotype generated by MOs against ENSDARG00000090815 can be rescued by co-injection with human *KCNJ10*.

Expression of the cloned full-length cDNA in oocytes induced  $K^+$ -selective currents that were indistinguishable from currents mediated by human *KCNJ10* (Fig. 1). We next established

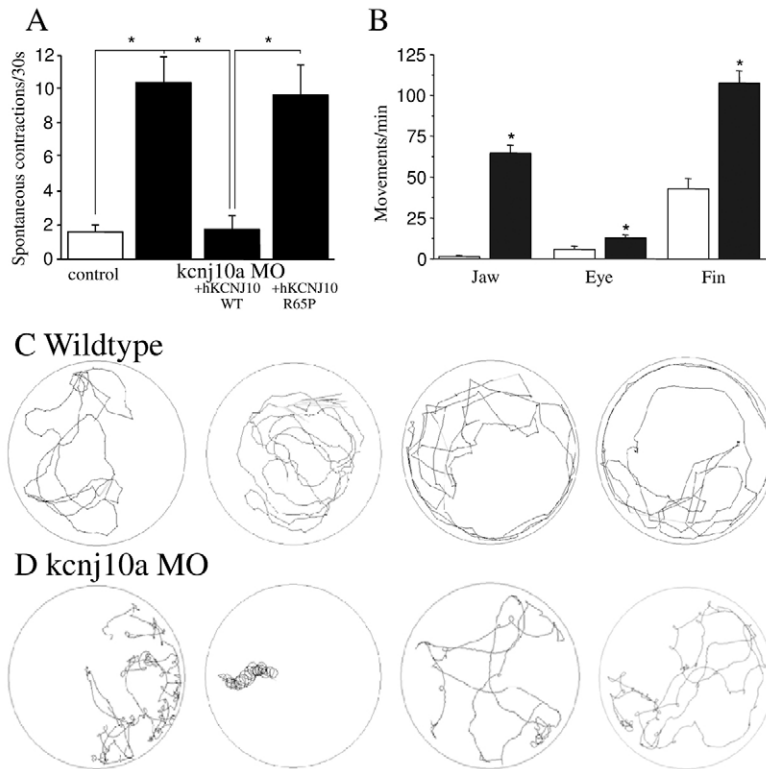


**Fig. 3. *kcnj10a* morphant ZF display movement defects.**

(A) Morphants showed an increased frequency of spontaneous contractions at 30 hpf, and this increase could be rescued by co-injection of normal human *KCNJ10* cRNA, but not R65P mutant cRNA ( $n=10-15$  per experimental condition). (B) At 120 hpf, we observed abnormal movements with a significantly higher frequency of jaw, eye and fin movements in *kcnj10a* morphants (black bars,  $n=7$ ) than in controls (white bars,  $n=5$ ). (C,D) Shown are 3-minute tracks from four WT (C) and four *kcnj10a* morphant (D) ZF at 120 hpf after being startled by touch. *kcnj10a* morphants (D) exhibit circling locomotion with frequent 'loops' around their vertical axis. \* $P<0.05$ .

expression of ZF *kcnj10a* in the main target organs of EAST syndrome: *kcnj10a* expression in the ZF cerebellum, otic vesicle, pronephros and retina (Fig. 2) recapitulated the expression of its mammalian orthologue in organs affected by EAST syndrome (Bockenbauer et al., 2009; Thompson et al., 2011). Its expression pattern in the ZF brain is particularly strong and consistent with glial expression in the fish CNS. In mammalian astrocytes and oligodendrocytes, *KCNJ10* helps siphon  $K^+$  from sites of high neuronal activity (Haj-Yasein et al., 2011), stabilising the neuronal resting membrane voltage. Expression in the ZF pronephros is weak. In humans, *KCNJ10* is expressed in the distal convoluted tubules, connecting tubules and early cortical collecting ducts (Reichold et al., 2010). Mouse expression of *KCNJ10* is more restricted and strain-specific (Lachheb et al., 2008; Reichold et al., 2010), suggesting that sites of expression might differ slightly in different species and strains. However, the function is conserved – in human and mouse kidney, *KCNJ10* is essential for maintaining extracellular levels of  $K^+$  required for  $Na^+/K^+$ -ATPase activity and therefore establishing the electrochemical gradient for  $Na^+$  and the hyperpolarised membrane voltage needed for epithelial ion transport, i.e. luminal  $Na^+$  reabsorption and basolateral chloride efflux (Bandulik et al., 2011) or maintenance of a proper and sufficient membrane voltage in excitable neuronal cells.

Injection of two different antisense MOs directed against *kcnj10a* resulted in several CNS phenotypes resembling EAST syndrome in humans: increased spontaneous contractions consistent with hyperexcitability (which probably leads to epilepsy), seizures, and several movement abnormalities consistent with ataxia. Spontaneous contractions (a readout that could be particularly easily quantified) were rescued by co-injection of human WT *KCNJ10*, but not with cRNA encoding for *KCNJ10* harbouring the

only partially functional EAST syndrome mutation, R65P. This proved the specificity of our antisense MOs, as well as functional equivalence of ZF *Kcnj10a* with the human protein in the CNS, suggesting that ZF *Kcnj10a* also functions to regulate glial extracellular  $K^+$  levels. Using this method to replace ZF *Kcnj10a* with normal or mutant versions of the human gene essentially allows us to 'humanise' the model. In addition to the brain phenotypes, there was evidence for kidney involvement in morphant fish, as shown by a dilated pronephric duct and delayed elimination of fluorescent dextran (Fig. 4). Thus, *kcnj10a* morphant fish represent, to our knowledge, the first genetic ZF model of a renal tubular disorder. Yet, whereas individuals with EAST syndrome exhibit salt loss, *kcnj10a* morphants retain water, reflecting the different role of the kidneys in this freshwater fish, namely to excrete water (Drummond, 2005). Recently, expression and function of *kcnj1* was investigated in ZF (Abbas et al., 2011). Mutations in the human orthologue cause another tubular disorder called Bartter syndrome type II (Kleta and Bockenbauer, 2006). However, the kidney function of *kcnj1* morphants was not specifically assessed.

EAST syndrome also includes sensorineural deafness, a feature that could not be confidently analysed in our model because the typical assessment for this is a rapid tail flick in response to auditory stimuli (Whitfield, 2002). Given the increased frequency of spontaneous tail flicks in the morphant fish, reliable analysis was not possible. However, the abnormal swimming behaviour is unlikely to be caused by lateral line dysfunction, because we did not see expression of *kcnj10a* in the lateral line organ.

ZF larval disease models are ideal for accelerating *in vivo* drug discovery providing that they have a phenotype that is easily automated. The model of EAST syndrome presented here displays

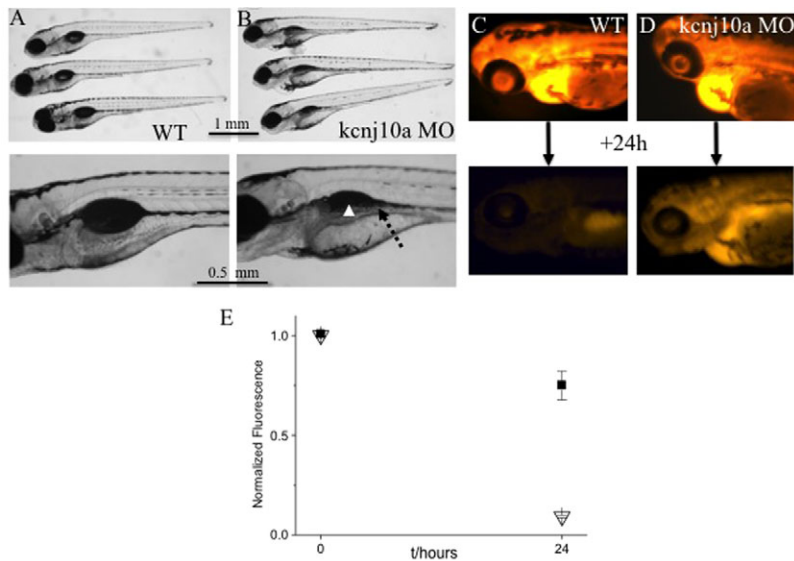


**Fig. 4. *kcnj10a* morphants have kidney defects.** (A,B) The upper images shows three 120-hpf WT larvae (A) and three *kcnj10a* morphants (B), some of which have pericardial edema. The lower image is an enlargement of the swim bladder and pronephric duct area. In morphants, the pronephric duct is visible because it is dilated (dotted arrow) and, although partially obscured by pigment, the swim bladder is not visible (arrowhead). (C,D) The upper and lower images show a 72-hpf WT (C) and a *kcnj10a* morphant (D) immediately after fluorescent dextran injection (upper image) and 24 hours later (lower image). Although baseline fluorescence immediately after injection was comparable in WT and morphant, there was significantly higher remaining fluorescence after 24 hours in morphant (D) compared with WT (C) ZF. (E) Graph of measured fluorescence in WT (triangles;  $n=9$ ) and morphant ZF (squares;  $n=12$ ).  $y$ -axis shows fluorescence intensity normalised for the baseline measurement in WT.  $x$ -axis shows time (hours).

locomotion defects such as increased spontaneous contractions, circling, bursts of speed and laboured movement that are easily detected using commercially available software (Baraban et al., 2005). Similarly, the presence or absence of kidney tubule dilation could be assessed quickly. Furthermore, because our model allows us to effectively 'humanise' KCNJ10 in ZF, such humanised ZF could be used to identify drugs that specifically modulate the function of human mutant KCNJ10, providing a unique opportunity to screen pharmacological agents for activity on human mutant KCNJ10 and to subsequently personalise treatments.

In the UK, and in many countries worldwide, procedures on ZF up to 120 hpf are considered ethically preferable over work on newborn mammals, and are therefore not regulated. Our ZF epilepsy model is a replacement model offering additional advantages over the use of knockout mice. Because *Kcnj10* knockout mice show white-matter vacuolisation and die within 2 weeks of life (Neusch et al., 2001), they are quite unlike individuals with EAST syndrome, who have no serious brain dysmorphology or premature death probably owing to preservation of residual function of KCNJ10 (Bockenbauer et al., 2009; Shi and Zhao, 2009). In fact, all EAST syndrome patients studied so far have at least one partially functional *KCNJ10* allele. Thus, ZF *kcnj10a* morphants better recapitulate EAST syndrome. Residual KCNJ10 function in individuals with EAST syndrome and these ZF *kcnj10a* morphants is likely to be sufficient for gross morphological brain development but not to prevent epilepsy, ataxia, sensorineural deafness and tubulopathy.

In summary, *kcnj10a* morphants, or *kcnj10a* morphants expressing mutated human *KCNJ10*, will accelerate the development of drugs targeting this channel and enable specific therapies to be developed whilst reducing the number of regulated animals that are used, providing a screening model to address the current lack of models required for the development of new drugs for EAST syndrome and its symptoms.

## MATERIALS AND METHODS

### Identification of ZF *kcnj10*

The ZF genome project is work in progress. Subsequent updates in the genome annotation can show new findings, which have to

be critically validated because bioinformatical annotations based on homology can easily create artifacts, especially with a highly homologous gene family such as the KCNJ potassium channels. Initially (assembly Zv7), a BLAST search using the human protein KCNJ10 as the query sequence and RefSeq as the target database produced XP\_001342993 (425 amino acids) as the best hit. The pairwise comparison confirmed the identity of XP\_001342993 and ENSDART00000006621.

Another BLAST search using UniProt as the target database produced Q1LUX0 (369 amino acids) as the best hit. When compared with ENSDART00000006621/XP\_001342993, it became clear that they are not the same [Score=301 bits (772), Expect=7e-80, Identities=146/320 (45%), Positives=212/320 (66%), Gaps=7/320 (2%)]. Visual inspection of the ZF Net (danRer5/July 2007) track, using the UCSC genome browser, suggested that the regions corresponding to the coding exons of human *KCNJ10* and *KCNJ9* are orthologous to ZF chromosome 10 fragments. The corresponding position on ZF chromosome 10 (which included ENSDART000000081978, a 333-amino-acid transcript) was considered to be orthologous to human chromosome 11 (hence the alignment was not reciprocal, because *KCNJ10* is located on human chromosome 1). The corresponding human region on chromosome 11 included *KCNJ5*.

The human KCNJ family was known to consist of 15 members: 1 to 16, 7 withdrawn (16 as per 2011, including *KCNJ18*). Eight of the members of this unique potassium channel family are present in reverse tandem orientation on the same individual chromosome (four pairs). After inspection of the corresponding genomic regions on the ZF Net track of the UCSC genome browser and multiple pairwise comparisons, we concluded that the genetic makeup of these potassium channels has structurally been conserved in evolution, so that the human 1-5 pair on chromosome 11 is equivalent to a ZF pair on chromosome 18; the human 16-2 pair on chromosome 17 is equivalent to a ZF pair on chromosome 12; the human 6-15 pair on chromosome 21 is equivalent to a ZF pair on chromosome 10; and the region of the human 9-10 pair on chromosome 1 is the equivalent of a ZF region situated on chromosome 7 – which includes ENSDART00000124851

(transcript corresponding to the ENSDARG00000090815 gene). However, the equivalent of *KCNJ9* previously and up to now was not captured in the region owing to the end of a sequencing contig. Apparently, the genome-wide duplication, supposed to have occurred in evolution during the emergence of teleosts, has not changed the overall genomic architecture of this unique *KCNJ* gene family.

Corroborating the available evidence, we concluded that ENSDART00000124851 was the ZF orthologue of human *KCNJ10* (uc001fuw.1, hg18). The pairwise P-BLAST alignment of the human (length 379 amino acids) and ZF (462 amino acids) protein sequences yielded a score of 25,916 (ID including gaps=65.0%, coverage of both=98.4%).

The upgrade of the ZF genomic assembly Zv7 to Zv8 changed the position of ENSDARG0000014697 from chromosome 7 to chromosome 8. A BLAST search using the nucleotide sequence of ENSDART0000006621 as the query sequence and HTGS (High Throughput Genomic Sequences) as the target database produced a perfect hit, CU914532.4 (described as ZF DNA sequence from clone CH1073-192C13 in linkage group 7). The ATG MO targeted against ENSDART00000124851 (5'-AGGGATAGGAGAGAGATGTTTCATTT-3') is a perfect match on the nucleotide sequence of CU914532.4. CU914532.4 matches 100% (BLAT) on chromosome 7 on Zv7/danRer5. Apparently, the chromosome 7 to chromosome 8 'shift' of ENSDART0000006621 between the Zv7 and Zv8 assemblies was due to an assembly error (due to a duplication-gap combination at that locus) that was fixed in Zv9/danRer7. ENSDARG0000014697 (which we here refer to as *kcnj10b*) is located on chromosome 2 in this assembly. The chromosome 7 ZF equivalent of *KCNJ10* (which we here refer to as *kcnj10a*) was renamed ENSDARG00000090815 (its transcript ENSDART00000124851 and the protein identifier ENSDARP00000106306).

#### Cloning of zebrafish *kcnj10a* and expression in *Xenopus* oocytes

ZF RNA was extracted from 120-hpf fish (TUP longfin) and purified using TRIZOL (Invitrogen, UK). RNA was then DNase I treated and purified using RNeasy columns (Qiagen, UK). cDNA was primed with polydT and transcribed with Superscript III (Invitrogen), all according to the manufacturers' instructions.

Primers 5'-ACATctcagATGACTTCAGCCACGCCCTTC-3' and 5'-ACATcttagaCTACAGTTACTGATGCGTACGC-3' (Integrated DNA Technologies, Belgium) were used to amplify (with 38 cycles) full-length ZF *kcnj10a* while attaching *XhoI* and *XbaI* restriction sites (lowercase in given sequence). The fragment was digested and ligated into empty pTLB cut with the same enzymes. Clones were fully sequenced and verified by direct sequencing of PCR fragments obtained using flanking primers on random hexamer-primed cDNA. The same was used to amplify and sequence part of the 5' and 3' untranslated regions. Primer sequences are available upon request. Heterologous expression in *Xenopus* oocytes was performed as described before (Zdebek et al., 2008). Briefly, ZF *kcnj10a* and human *KCNJ10* were transcribed from linearised pTLB constructs using the mMessage Machine Sp6 kit (Ambion, USA) according to the manufacturer's instructions, diluted as appropriate to allow injection of 2 or 5 ng cRNA into each *Xenopus* oocyte using a custom-made injector. Oocytes were incubated at 17°C for 1-2 days in ND96 containing (in mM) 96

NaCl, 2 KCl, 1.8 CaCl<sub>2</sub>·2H<sub>2</sub>O, 1 MgCl<sub>2</sub>·6H<sub>2</sub>O, 5 HEPES, pH 7.5, and subjected to two-electrode voltage clamp using a modified TEC01C amplifier (npi electronic GmbH, Germany). To increase *KCNJ10*-specific currents and to investigate rectification under symmetrical K<sup>+</sup>, 96 mM NaCl was replaced by 96 mM KCl in ND96. For barium inhibition experiments, 100 μM BaCl<sub>2</sub> was added to the bath solution. Oocytes were held at -30 mV and clamped from -100 to +60 mV in 20 mV increments. Two batches were analysed and results averaged using Origin software (OriginLab, USA).

#### In situ hybridisation

*In situ* hybridisation was performed as described before (Macdonald et al., 1994). A 600 bp fragment of the *kcnj10a* cDNA was generated by PCR from cloned full-length *kcnj10a* using primers (Invitrogen) that add T3 and T7 promoter sequences (lowercase) to the ends of the PCR product. T3-antisense primer: 5'-aattaacctactaaagg-AGGCTACATTCCTCTGGTCCAGACGC-3'; T7-sense primer: 5'-taatacagactactataggTCCAAAGATGGGCGGAGCAACGTT-CG-3'. Transcription using T3 polymerase produced antisense RNA and T7 polymerase produced sense RNA.

For *kcnj10b*, c1-c340 of the cDNA was cloned into pBluescript, via *XhoI* and *XbaI*, sequence-verified and digested, and transcribed as stated: antisense probe: *XhoI* and T7; sense probe: *XbaI* and T3.

ZF ranging from the 128-cell stage to 120 hpf were hybridised with either the sense (control) or antisense probe and developed for the same duration. Brightfield and DIC (differential interference contrast) images were taken with a Leica DM4000B or Zeiss Axiovert microscope and digital camera using LAS software (Leica), or with a Nikon SMZ15000 microscope, Digital Sight camera (Nikon) and supplied software. ZF were impregnated with 30% sucrose/1×PBS for 2-3 hours, mounted individually in TissueTek O.C.T. (VWR, UK) and snap-frozen on dry ice. Each ZF was transverse-sectioned into 10-μm slices using a cryostat OTF5000 (Bright Instrument Company Ltd, UK), transferred onto Superfrost PLUS slides (VWR) and imaged. Images were processed in Photoshop CS (Adobe, USA) using the same image acquisition settings and manipulations on antisense and sense ZF of the same age.

#### Zebrafish lines and husbandry

Embryos were obtained by natural spawning from WT ZF (TupLongfin). All ZF were reared and staged according to standard procedures.

#### Generation of morphants

MOs (Gene Tools, USA) targeting the start ATG (5'-AGGGATAG-GAGAGAGATGTTTCATTT-3') or a splice site (5'-AATTGTGAGAGCTATACCTTGCGGA-3') of ZF *kcnj10a*, the ATG of *kcnj10b* (5'-CCGAGGTCATCTAGGGAAGAAAGAC-3'), *p53* (5'-GCGCCATTGCTTTGCAAGAATTG-3'), and a negative control MO directed against a human β-globin intron mutation (5'-CCTCTTACCTCAGTTACAATTTATA-3'), were diluted into MO buffer containing (in mM) 58 NaCl, 0.7 KCl, 0.4 MgSO<sub>4</sub>, 0.6 Ca(NO<sub>3</sub>)<sub>2</sub>, 5 HEPES, pH 7.6, and injected into one- to two-cell-stage ZF, which were raised at 28°C.

#### RT-PCR of *kcnj10a*

Total RNA extraction of 48-hpf WT and *kcnj10a* splice site MO (2 ng)-injected ZF was performed as stated, except that random

primers were used during cDNA synthesis. A *kcnj10a* cDNA fragment was PCR-amplified using the following primers (in exon 1 and 4, respectively): Forward, 5'-ACATctcgagATGACTTC-AGCCACGCCCTTC-3'; Reverse, 5'-ACA TcttagaAGGCTA-CATTCTCTGGTCCAGACGC-3'.

1/20 of the Superscript III transcript was PCR amplified using Phusion polymerase HF, at an annealing temperature of 62°C and 38 cycles according to the manufacturer's instructions. The resulting product was visualised, gel purified using High Pure (Roche) and an aliquot digested with *Bgl*II (Fermentas).

### Spontaneous contraction analysis and rescue

At 30 hpf, the ZF, still in their chorion, were placed in individual wells of a 12-well plate and equilibrated for 3 minutes. The number of complete body contractions each ZF made in a 30 second period was counted. 10-15 ZF were counted for each treatment and the average number of complete contractions calculated. For rescue experiments, 50 pg human WT or R65P mutant *KCNJ10* cRNA was co-injected with 0.5 ng of *kcnj10a* splice site MO. For experiments employing the *p53* MO in concert with the *kcnj10a* or *kcnj10b* MO, a video of a 180 second period was made using Media Recorder (Noldus) and a digital video camera (30 frames per second) on a Nikon SMZ1500 microscope. The tail flicks were subsequently counted from the videos and the data was placed in Prism (GraphPad) to generate graphs and perform statistical analysis (unpaired two-tailed Mann-Whitney *U*-test of all pairwise combinations).

### Movement analysis

120-hpf ZF were equilibrated in a 70 mm glass dish, the ZF were started by touching with a fine pipette and 3-minute movies were recorded using a Zebibox motion tracker and motion paths reconstructed using Videotrack software (Viewpoint, France). At least ten different ZF were used for each condition.

Alternatively, an individual 120-hpf ZF was placed in 50 µl of aquarium water (AW) within a single well of a 96-well plate, mounted on the stage of a brightfield microscope. 170-second video recordings of individual fish were obtained at a frame rate of 20 per second. Chamber temperature was kept constant at 28°C and humidified.

In a further method, an individual 120-hpf ZF was placed in 50 µl of AW within a single well of a 96-well plate on a brightfield SMZ1500 microscope and videoed using a digital video camera (30 frames per second) and MediaRecorder software (Noldus). Locomotion was tracked using Ethovision XT software (Noldus). Data was placed in Prism (GraphPad) to generate graphs and perform statistical analysis (unpaired two-tailed Mann-Whitney *U*-test of all pairwise combinations).

### Renal function assessment

To investigate renal function, 72-hpf WT and *kcnj10a* morphant ZF were anaesthetised and 1 nl of 1% rhodamine-labelled 10 kDa dextran (Sigma, UK) was microinjected into the pericardium, as described (Hentschel et al., 2007). The following day, the amount of residual fluorescence in the heart was compared with the amount immediately after injection. Decreased fluorescence correlates with clearance of the dextran by the kidneys.

### Immunohistochemistry

Larvae were processed for anti-acetylated  $\alpha$ -tubulin (Sigma, UK) immunohistochemistry as previously described (Concha et al., 2000). Brightfield images were taken with a digital camera using LAS software (Leica) on a DM4000B microscope. Images were processed in Photoshop CS (Adobe, USA) using the same image-acquisition settings and manipulations.

### Statistical analysis

Statistical analysis was performed in Origin (OriginLab, USA) with the two-sided unpaired or paired Student's *t*-test.  $P < 0.05$  was considered significant.

### Experimental subjects

All ZF experiments were approved by the Royal Veterinary College, UCL and the UK Home Office.

### ACKNOWLEDGEMENTS

We thank Steve W. Wilson and Anukampa Barth at UCL for advice and access to specific equipment, the UCL workshops for help with instrument design, and Andrew Hibbert (RVC Imaging Unit) for advice on digital movies.

### COMPETING INTERESTS

The authors declare that they do not have any competing or financial interests.

### AUTHOR CONTRIBUTIONS

All authors reviewed the data, co-wrote and reviewed the manuscript. F.M. and M.M. generated morpholino knockdown ZF, performed RT-PCR and free swimming locomotion assays, and sectioned embryos. J.T. designed morpholinos, generated morpholino knockdown ZF, and performed rescue experiments, locomotion assays and the dextran excretion assay. H.C.S. performed all bioinformatical work needed for successful cloning. A.A.Z. cloned ZF *kcnj10a* and *kcnj10b*, performed electrophysiology in oocytes, and generated human *KCNJ10* cRNA for rescue experiments. P.L.B. supervised J.T. and provided access to the zebrafish core facility. R.K. and D.B. initiated and developed this study, and provided funding and overall project supervision and management at UCL. C.R. received funding and provided supervision for F.M. and M.M., and generated and analysed the *in situ* hybridisation and immunohistochemistry data.

### FUNDING

Funding for F.M. was provided via a doctoral training grant from the Royal Veterinary College (RVC) (to C.R.). Funding for consumables and animals at the RVC (to C.R. and F.M.) was provided by an RVC start-up grant (to C.R.). UCL work was supported by grants from the David and Elaine Potter Charitable Foundation and Grocers' Charity (to R.K.), St Peter's Trust for Kidney, Bladder and Prostate Research (to A.A.Z., D.B. and R.K.), Kids Kidney Research and Garfield Weston Foundation (to D.B. and R.K.), and by the EU FP7 program (EUREnOmics, grant agreement number 305608 to D.B. and R.K.). A.A.Z. received additional support from the Peter Samuel Trust Fund. J.T. was supported by an MRC PhD studentship. D.B. is a HEFCE Clinical Senior Lecturer.

### SUPPLEMENTARY MATERIAL

Supplementary material for this article is available at <http://dmm.biologists.org/lookup/suppl/doi:10.1242/dmm.009480/-/DC1>

### REFERENCES

- Abbas, L., Hajjhashemi, S., Stead, L. F., Cooper, G. J., Ware, T. L., Munsey, T. S., Whitfield, T. T. and White, S. J. (2011). Functional and developmental expression of a zebrafish Kir1.1 (ROMK) potassium channel homologue *Kcnj1*. *J. Physiol.* **589**, 1489-1503.
- Bandulik, S., Schmidt, K., Bockenhauer, D., Zdebik, A. A., Humberg, E., Kleta, R., Warth, R. and Reichold, M. (2011). The salt-wasting phenotype of EAST syndrome, a disease with multifaceted symptoms linked to the KCNJ10 K<sup>+</sup> channel. *Pflügers Arch.* **461**, 423-435.
- Baraban, S. C., Taylor, M. R., Castro, P. A. and Baier, H. (2005). Pentylentetrazole induced changes in zebrafish behavior, neural activity and *c-fos* expression. *Neuroscience* **131**, 759-768.
- Bleich, M. (2009). Membrane physiology – bridging the gap between medical disciplines. *N. Engl. J. Med.* **360**, 2012-2014.
- Bockenhauer, D., Feather, S., Stanescu, H. C., Bandulik, S., Zdebik, A. A., Reichold, M., Tobin, J., Lieberer, E., Sterner, C., Landouge, G. et al. (2009). Epilepsy, ataxia,

- sensorineural deafness, tubulopathy, and KCNJ10 mutations. *N. Engl. J. Med.* **360**, 1960-1970.
- Concha, M. L., Burdine, R. D., Russell, C., Schier, A. F. and Wilson, S. W.** (2000). A nodal signaling pathway regulates the laterality of neuroanatomical asymmetries in the zebrafish forebrain. *Neuron* **28**, 399-409.
- Drummond, I. A.** (2005). Kidney development and disease in the zebrafish. *J. Am. Soc. Nephrol.* **16**, 299-304.
- Haj-Yasein, N. N., Jensen, V., Vindedal, G. F., Gundersen, G. A., Klungland, A., Ottersen, O. P., Hvalby, O. and Nagelhus, E. A.** (2011). Evidence that compromised K(+) spatial buffering contributes to the epileptogenic effect of mutations in the human kir4.1 gene (KCNJ10). *Glia* **59**, 1635-1642.
- Hentschel, D. M., Mengel, M., Boehme, L., Liebsch, F., Albertin, C., Bonventre, J. V., Haller, H. and Schiffer, M.** (2007). Rapid screening of glomerular slit diaphragm integrity in larval zebrafish. *Am. J. Physiol. Renal Physiol.* **293**, F1746-F1750.
- Hibino, H., Horio, Y., Inanobe, A., Doi, K., Ito, M., Yamada, M., Gotow, T., Uchiyama, Y., Kawamura, M., Kubo, T. et al.** (1997). An ATP-dependent inwardly rectifying potassium channel, KAB-2 (Kir4.1), in cochlear stria vascularis of inner ear: its specific subcellular localization and correlation with the formation of endocochlear potential. *J. Neurosci.* **17**, 4711-4721.
- Hibino, H., Horio, Y., Fujita, A., Inanobe, A., Doi, K., Gotow, T., Uchiyama, Y., Kubo, T. and Kurachi, Y.** (1999). Expression of an inwardly rectifying K(+) channel, Kir4.1, in satellite cells of rat cochlear ganglia. *Am. J. Physiol.* **277**, C638-C644.
- Hortopan, G. A., Dinday, M. T. and Baraban, S. C.** (2010a). Spontaneous seizures and altered gene expression in GABA signaling pathways in a mind bomb mutant zebrafish. *J. Neurosci.* **30**, 13718-13728.
- Hortopan, G. A., Dinday, M. T. and Baraban, S. C.** (2010b). Zebrafish as a model for studying genetic aspects of epilepsy. *Dis. Model. Mech.* **3**, 144-148.
- Kleta, R. and Bockenhauer, D.** (2006). Bartter syndromes and other salt-losing tubulopathies. *Nephron Physiol.* **104**, p73-p80.
- Lachheb, S., Cluzeaud, F., Bens, M., Genete, M., Hibino, H., Lourdel, S., Kurachi, Y., Vandewalle, A., Teulon, J. and Paulais, M.** (2008). Kir4.1/Kir5.1 channel forms the major K+ channel in the basolateral membrane of mouse renal collecting duct principal cells. *Am. J. Physiol. Renal Physiol.* **294**, F1398-F1407.
- Macdonald, R., Xu, Q., Barth, K. A., Mikkola, I., Holder, N., Fjose, A., Krauss, S. and Wilson, S. W.** (1994). Regulatory gene expression boundaries demarcate sites of neuronal differentiation in the embryonic zebrafish forebrain. *Neuron* **13**, 1039-1053.
- Marcus, R. C. and Easter, S. S., Jr** (1995). Expression of glial fibrillary acidic protein and its relation to tract formation in embryonic zebrafish (*Danio rerio*). *J. Comp. Neurol.* **359**, 365-381.
- Mueller, T. and Wullmann, M. F.** (2005). *Atlas of Early Zebrafish Brain Development*. Amsterdam: Elsevier.
- Neusch, C., Rozengurt, N., Jacobs, R. E., Lester, H. A. and Kofuji, P.** (2001). Kir4.1 potassium channel subunit is crucial for oligodendrocyte development and *in vivo* myelination. *J. Neurosci.* **21**, 5429-5438.
- Olsen, M. L. and Sontheimer, H.** (2008). Functional implications for Kir4.1 channels in glial biology: from K+ buffering to cell differentiation. *J. Neurochem.* **107**, 589-601.
- Parg, C., Seng, W. L., Semino, C. and McGrath, P.** (2002). Zebrafish: a preclinical model for drug screening. *Assay Drug Dev. Technol.* **1**, 41-48.
- Reichold, M., Zdebik, A. A., Lieberer, E., Rapedius, M., Schmidt, K., Bandulik, S., Sterner, C., Tegtmeyer, I., Penton, D., Baukrowitz, T. et al.** (2010). KCNJ10 gene mutations causing EAST syndrome (epilepsy, ataxia, sensorineural deafness, and tubulopathy) disrupt channel function. *Proc. Natl. Acad. Sci. USA* **107**, 14490-14495.
- Rozengurt, N., Lopez, I., Chiu, C.-S., Kofuji, P., Lester, H. A. and Neusch, C.** (2003). Time course of inner ear degeneration and deafness in mice lacking the Kir4.1 potassium channel subunit. *Hear. Res.* **177**, 71-80.
- Scholl, U. I., Choi, M., Liu, T., Ramaekers, V. T., Häusler, M. G., Grimmer, J., Tobe, S. W., Farhi, A., Nelson-Williams, C. and Lifton, R. P.** (2009). Seizures, sensorineural deafness, ataxia, mental retardation, and electrolyte imbalance (SeSAME syndrome) caused by mutations in KCNJ10. *Proc. Natl. Acad. Sci. USA* **106**, 5842-5847.
- Shi, M. and Zhao, G.** (2009). The EAST syndrome and KCNJ10 mutations. *N. Engl. J. Med.* **361**, 630, author reply 630-631.
- Thompson, D. A., Feather, S., Stanescu, H. C., Freudenthal, B., Zdebik, A. A., Warth, R., Ognjanovic, M., Hulton, S. A., Wassmer, E., van't Hoff, W. et al.** (2011). Altered electroretinograms in patients with KCNJ10 mutations and EAST syndrome. *J. Physiol.* **589**, 1681-1689.
- Whitfield, T. T.** (2002). Zebrafish as a model for hearing and deafness. *J. Neurobiol.* **53**, 157-171.
- Zdebik, A. A., Zifarelli, G., Bergsdorf, E. Y., Soliani, P., Scheel, O., Jentsch, T. J. and Pusch, M.** (2008). Determinants of anion-proton coupling in mammalian endosomal CLC proteins. *J. Biol. Chem.* **283**, 4219-4227.